Solar Energy Materials & Solar Cells 93 (2009) 167–175

Contents lists available at ScienceDirect

Solar Energy Materials & Solar Cells

journal homepage: www.elsevier.com/locate/solmat

Sliver cells in thermophotovoltaic systems

N.N. Lal [a,*], A.W. Blakers [b]

[a] Department of Physics, College of Science, The Australian National University, Canberra, ACT 0200, Australia
[b] Centre for Sustainable Energy Systems, College of Engineering and Computer Science, The Australian National University, Canberra, ACT 0200, Australia

ARTICLE INFO

Article history:
Received 1 May 2008
Received in revised form
11 September 2008
Accepted 16 September 2008
Available online 29 November 2008

Keywords:
Thermophotovoltaics
Sliver cells
Photovoltaic modelling

ABSTRACT

Previous modelling has indicated that silicon solar cells should be thinner than 100 μm to be optimal for use in thermophotovoltaic (TPV) systems. Sliver cells are a novel type of thin photovoltaic cells fabricated from single crystal semiconductor wafers, with their contacts at the edges of the cell. A computational model was constructed to examine and compare the performance of silicon sliver cells with silicon conventional back-contact cells in TPV systems. Within the range of parameters investigated it was found that the lateral carrier transport resistance of sliver cell geometries limits their power output relative to conventional cells in TPV systems. In practical systems, the efficiencies are comparable.

1. Introduction

1.1. Thermophotovoltaics

Thermophotovoltaic (TPV) systems are direct conversion heat engines that use photovoltaic cells to generate electricity from the radiant energy emitted from a heated object [1,2]. In TPV systems, an object, typically a grey body or selective emitter, is heated to temperatures typically higher than 1000 K; 1300–2000 K is considered the practical range [3]. The resulting radiation is collected by surrounding photovoltaic cells (Fig. 1).

Photons not absorbed by the cells are reflected back to the emitter by a mirror behind the cells, thus conserving the emitter energy. TPV geometries are substantially different from those of conventional flat-panel photovoltaic modules.

1.2. Current TPV systems

The main technical limiting factors of TPV systems are spectral filtering, cell conversion efficiency, adequate systems modelling and thermal management [3,4]. An important commercial limitation is the difficulty of accessing suitable low-cost efficient solar cells. Ideally, TPV cells would have a bandgap of 0.6–0.9 eV to take account of the lower temperature of a practical TPV emitter (1300–2000 K) compared with the sun. This should be combined with mature high efficiency fabrication technology and mass production to achieve low cost. Silicon solar cells have low cost (~\$0.10/cm^2) and high efficiency (>20% under sunlight). However, the bandgap (1.1 eV) is higher than optimum.

An early theoretical study by Swanson [5] indicated that the optimal thickness for silicon cells in TPV systems was ~25 μm. The thickness of conventional silicon cells is currently ~200 μm, with the possibility of 100 μm thicknesses for high-value applications. Thicknesses below 100 μm are currently difficult to manufacture using conventional techniques.

1.3. Sliver cells

Sliver technology is a novel method of fabricating highly efficient (>20%) thin silicon solar cells [6].

Sliver cells are processed within the wafer and are later extracted to form many individual cells [7]. Sliver cells are thin, flexible and bifacial. Importantly, they have thin (1 μm) metal contacts on the edges of the cell rather than on one or both faces, as illustrated in Fig. 2.

Sliver cells can be made up to a factor of 10 times thinner than conventional cells. Current sliver cells have typical length 50–120 mm, width of 0.5–2 mm and thickness 20–100 μm. Future sliver width could be decreased to ~300 μm using current manufacturing techniques. The minimum sliver width modelled in this project was 300 μm. Current work is extending this modelling to widths of <200 μm, discussed further in Section 3.2.

Bifacial response facilitates photon recycling in TPV systems by allowing unimpeded transmission of unabsorbed light through the rear surface of the cell to a mirror, and back through the cell to the thermal emitter.

* Corresponding author. Tel.:+61 8 9245 4994.
E-mail addresses: nirajlal@gmail.com (N.N. Lal), andrew.blakers@anu.edu.au (A.W. Blakers).

0927-0248/\$ - see front matter © 2008 Elsevier B.V. All rights reserved.
doi:10.1016/j.solmat.2008.09.060

Thinness causes a reduction in parasitic free-carrier absorption of infrared light, allowing an increased proportion of sub-bandgap photons to be able to be recycled back to the TPV emitter. Very thin electrical contacts on the edges of the cell reduce parasitic reflection and absorption from the cell surface, and allow more light to be incident on the active cell area. Metal contacts on the edges also allow for easy thermal contact to a heat sink along the entire rear surface of the cell while maintaining electrical isolation, an important consideration for TPV systems. In addition, edge-to-edge series interconnection of narrow sliver cells allows voltage to be easily built up at a rate of around 10 V per linear cm in the lateral direction, with correspondingly low current, reducing circuit-resistive losses.

Edge contacts to the cell results in a different transport resistance geometry compared to conventional cells. Instead of one or both charge carriers being transported vertically to the rear surface, as in conventional or rear contact cells, respectively, both charge carriers are transported laterally (in opposite directions) across the cell width. This is observed to be of considerable importance for the output power of sliver cells operating at the high illumination densities of TPV systems [7].

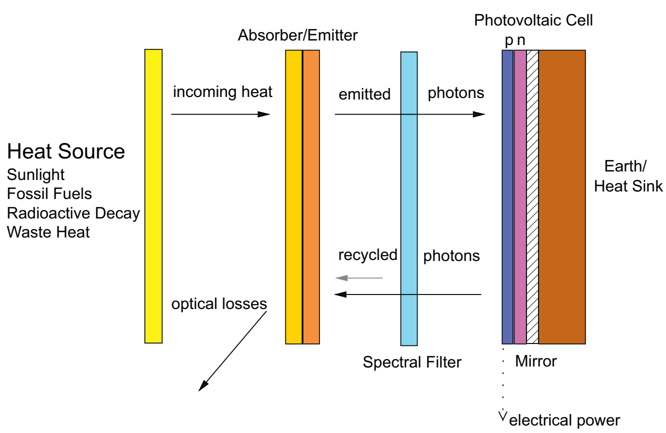

Fig. 1. Schematic diagram of a thermophotovoltaic system.

Sliver cells have applications in many different photovoltaic systems [6]. We present a modelling investigation into the application of silicon sliver cells in TPV systems, and compare their performance with state-of-the-art conventional silicon back-contact cells.

2. Methods

A computational model was developed to investigate the effects of cell thickness and geometry in realistic TPV systems. Sliver cells were compared with high-performance conventional back-contact solar cells. A number of detailed semiconductor device models are available that numerically solve the fully coupled set of nonlinear semiconductor transport equations. While well suited to the detailed examination of photovoltaic cell charge transport, such models are cumbersome to apply to the multiple photon reflections and emitter re-absorptions that are present in TPV systems [8].

Monte Carlo modelling allows the extended tracing of photons in two and three dimensions. Monte Carlo methods are well suited to modelling TPV systems; they are able to model the multiple reflections within TPV systems and heat conduction from the cell. With this advantage, however, comes additional complexity and computational cost [8]. In light of this cost, and for the simple and dedicated analysis of sliver cells in TPV systems, a linear model was chosen for this project. The constructed model, presented below, is similar to a simplified Monte Carlo model in that the histories of a number of photons are tracked. The key difference is that the assumed paths of photons are restricted to one dimension, resulting in the angular dependence of absorption, reflection and transmission processes being neglected. Since a TPV system relies on efficient photon recycling between the thermal emitter and the cell/mirror, one-dimensional photon trajectories are essential to minimize photon scatter. A solar cell designed for a TPV system will have very smooth parallel faces without light

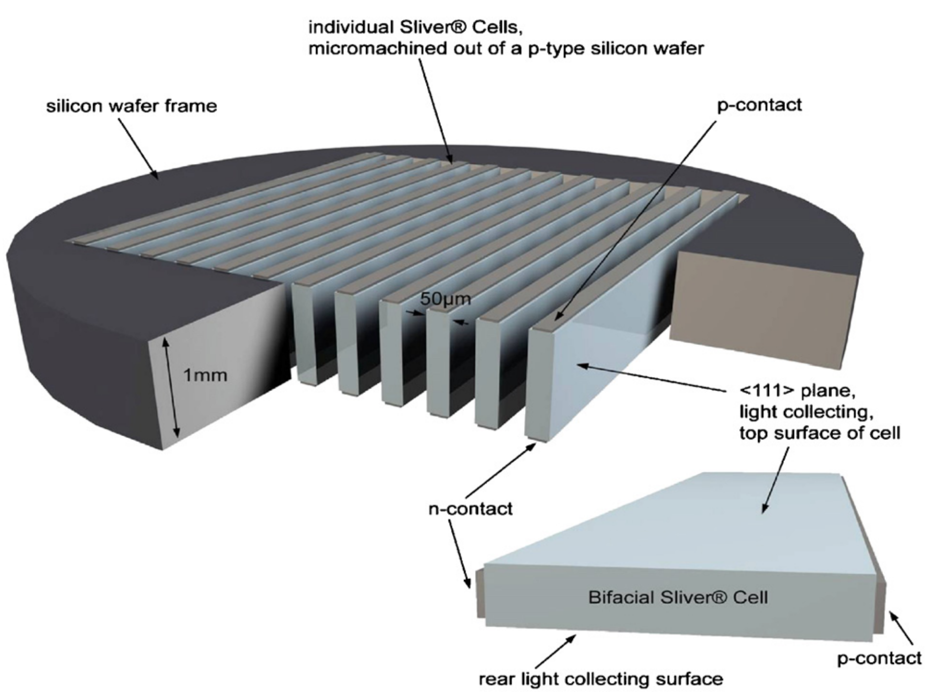

Fig. 2. Diagram of sliver cell fabrication [7].

trapping features, and minimal scattering of light from metal contacts.

The two-dimensional carrier resistive losses of sliver cells are still able to be modelled since it is only the path of *photons* that are restricted to one dimension (Fig. 3).

For our primary aim of comparing sliver versus conventional cells in TPV systems we have focused on those variables that affect each cell type differently, such as cell thickness and incident spectra. Variables such as mirror reflectance, cell temperature and optical losses have a significant effect on system efficiency, but are found to affect both sliver and conventional cell performance almost identically. As a result, we have attempted to set external variables at excellent but achievable levels.

Mirror reflectivity data were obtained from the secondary mirror of an infrared telescope [9] and cell temperatures were set to 20° above ambient (318 K). The effects of mirror reflectivity, cell temperature and optical losses on realistic TPV system efficiencies are discussed in Section 3.3.

Data for the antireflectance coating of both conventional and sliver cells were obtained from experimental reflectance data of a dual layer MgF_2/ZnS antireflection coating developed by Boufhas et al. [10]. The optimization of antireflection coating is an important issue for TPV systems [11], though not a primary focus for this study. The antireflection coating chosen had high reflectance for the blue end of the spectrum (where TPV emission is also low), and a reflection minimum for wavelengths of 800–1000 nm. Reflection of sub-bandgap wavelengths in our modelled TPV system was provided by placing the mirror behind the cells.

Modelling was undertaken with silicon as the semiconductor material due to the availability of relatively very low-cost solar cells compared with other candidate materials, even though silicon is not an ideal semiconductor for TPV cells due to its relatively high bandgap of 1.12 eV. The investigation provided an indication of the feasibility of thin silicon cells in TPV systems. Gallium antimonide with an energy bandgap of 0.72 eV is the material currently being considered for TPV cells by most researchers due to its superior absorption response for lower blackbody temperatures.

Silicon is a relatively poor absorber of infrared light, and so, in the absence of light trapping, thick cells are required to maximize light absorption. However, this is associated with decreased IQE and increased parasitic-free carrier absorption and volume recombination. The material parameters for silicon photovoltaic cells are well established. Accurate device modelling with these parameters enabled a detailed examination of cell performance.

Charge carrier transport series resistance losses for both conventional and sliver cells is significant for TPV applications because of the high concentration of light under optimum conditions. Carrier transport resistance losses are found through $P_{\text{loss}} = \int_0^x I^2\,\mathrm{d}R$, where x is the distance charge carriers must travel, and $\mathrm{d}R = (\rho\,\mathrm{d}x/Area)$. Here ρ is the resistivity of the semiconductor with units of (Ω cm), and the area is the cross-sectional area through which the carriers must travel.

For conventional back-contact cells the charge carriers are transported approximately vertically through the cell (Fig. 4). Most photon absorption occurs relatively near the upper surface, requiring transport of electrons and holes through most of the wafer thickness, placing strict requirements upon high carrier lifetimes. The percentage power loss (neglecting conductivity modulation) can be calculated using standard methods as $P_{\text{conventionloss}}\% = (\rho H J_{\text{mp}}/V_{\text{mp}})$ [12]. Here J_{mp} and V_{mp} are the current density and voltage of the cell, respectively, at maximum power, and the resistive power loss is observed to depend linearly on the cell thickness, H. Conductivity modulation reduces this loss.

For p-type sliver cells, both electrons and holes are transported laterally across the sliver cell width (in opposite directions). The resistive loss (in terms of percentage power loss) can be calculated using standard methods used for determining lateral resistive loss in conventional solar cells [12] and is approximately given by $P_{\text{sliverloss}}\% = (\rho W^2 J_{\text{mp}}/3HV_{\text{mp}})$, with an equivalent expression for the emitter with $R_\square = \rho/h$. For the emitter resistance, h is the thickness of the emitter region as opposed to H the thickness of the bulk. $R_\square$ is the resistivity per unit thickness, with units of $\Omega/\square$.

The resistive power loss for sliver cells is observed to depend on the square of the cell width (W), the emitter sheet resistance (for electrons) and the inverse of cell thickness (for holes).

The difference between the transport resistance losses for the two cell types proved to be significant in this project.

In the TPV model, J_{sc} was calculated from the absorption of above-bandgap photons (adjusted for optical losses from the cell contacts and mirror absorption); V_{oc} was calculated from the solar cell equation and the recombination rate J_0; and the fill factor was calculated using the empirical expression from Green [12]. The surface recombination current $J_{0\text{s}}$ was set in accordance with the best current sliver cells, which is equivalent to a level that, neglecting all other recombination, limited sliver cell V_{oc} to

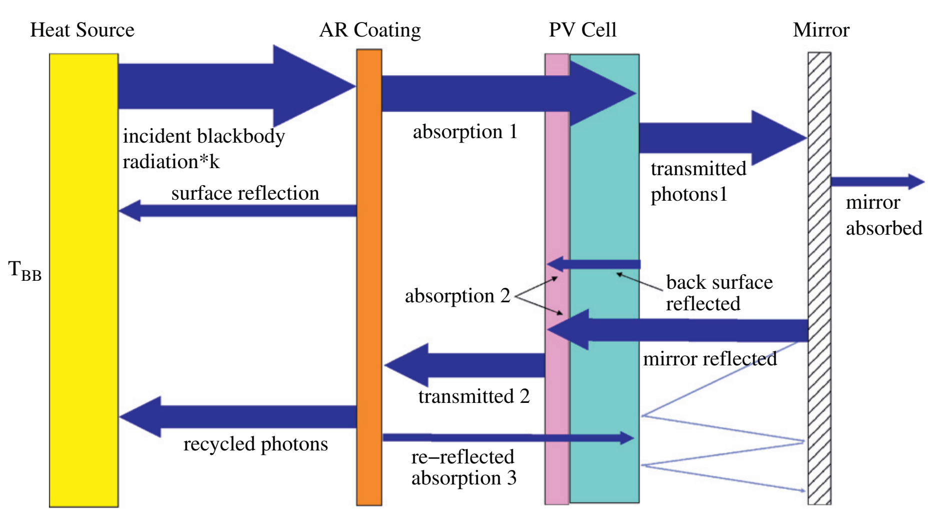

Fig. 3. Schematic diagram of the thermophotovoltaic computational model.

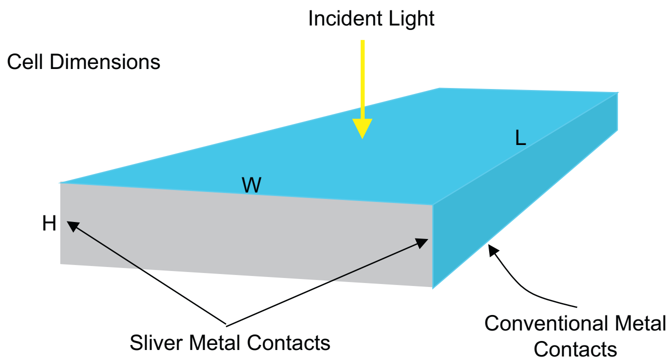

Fig. 4. Cell contact location.

700 mV. Conventional cell J_{0s} was set to half the sliver value, reflecting the greater ease of passivating the easily accessible surfaces of conventional cells. J_{0b} and J_{0e}, the bulk and emitter current densities, respectively, were found using the standard analytical expressions found in Green [12]. Bulk resistivity and emitter sheet resistance were set to ensure internal quantum efficiency was greater than 99% for a given thickness, in accordance with current practice in designing sliver cells. These values were found using PC1D, a detailed semiconductor modelling program developed at Sandia National Laboratories that solves the fully coupled set of nonlinear semiconductor transport equations in one dimension [13].

Blackbody temperatures in this project were investigated from 1200–4200 K. This represents the range of practical TPV emitter temperatures, with an extension to higher temperatures that give an indication of silicon's response to spectra more suited to its bandgap.

The cells were modelled as a shell completely surrounding the emitter. That is, the efficiencies presented do not take into account the practical optical losses associated with gaps between the shell of cells surrounding the thermal emitter. In a realistic TPV system, such optical losses amounting to perhaps 10% will be present.

A number of sources of error arising from modelling simplifications were present within our calculations. Material resistivity was set to ensure >99% IQE for a given thickness. However, for cell thicknesses larger than 500 μm, realistic IQE will be reduced to around 96% due to inadequate diffusion length. In addition, recombination at the back surface contacts in conventional cells could be significant, but was neglected.

The main method of validation for the analytical cell performance calculations of the constructed model was to use PC1D. PC1D is well suited to the analysis of most photovoltaic cells, since most processes within the cells are essentially one-dimensional; however, PC1D is unable to model the two-dimensional lateral carrier transport of sliver cells. The agreement between PC1D and the analytical model was to within 1% across the range of parameters investigated. With the consideration of internal quantum efficiency and surface recombination density, and also with consideration of the extrapolation of TPV component parameters, the uncertainty of the TPV model is presented as ±4% for cell thicknesses in the range 10–500 μm and ±6% for cell thicknesses 500–1000 μm.

3. Results and discussion

3.1. Conventional cells

A back-contact cell with a large (⩾cell thickness) minority carrier diffusion length was analysed in a TPV system with different cell thicknesses, and for a range of blackbody temperatures. The cell was modelled with a double-layer antireflection coating, and negligible absorption of light at the back-contacts. The latter assumption could be difficult to achieve in practice. Incident power density on the cell was optimized for each blackbody temperature and cell thickness. This is achieved in practice by adjusting the distance between the cells and the emitter. The area of cells required for each thermal emitter temperature is inversely proportional to the incident power density.

The efficiency of the TPV system is considered as the ratio of electrical power output to the power required to keep the blackbody at a constant temperature:

$$\eta_{\mathrm{TPV}} = \frac{J_{sc} \times V_{oc} \times FF}{\text{Power radiated} - \text{Power returned}} \tag{3.1}$$

The denominator indicates a significant feature of TPV systems; it is constituted not only by the power radiated by the blackbody, but also by the power returned to the emitter, since most photons not absorbed are able to be recycled (Fig. 5).

An efficiency maximum of (38±2)% is observed in the model. The maximum occurs at ~3000 K, which is substantially higher than the current range of practical TPV temperatures of approximately 1200–2400 K. The Carnot efficiency at 3000 K is ~90%. At a practical TPV temperature of 2000 K, the modelled efficiency for conventional silicon cells is ~27%. Presented efficiencies are for the idealised TPV cell component, modelled to be completely surrounding the radiating emitter. The figures incorporate neither optical losses due to TPV system design nor efficiency losses due to the power required for cell cooling; further discussion of net TPV system efficiency is presented in Section 3.3.

Through the use of Wien's Law, and from the difference in bandgaps of silicon (1.12 eV) and gallium antimonide (0.72 eV), we can estimate to first order that gallium antimonide cells would perform similar to silicon cells at blackbody temperatures ~900 K less than those for silicon. The cost and manufacturing advantages of silicon cells would need to offset the potentially higher efficiencies available from lower bandgap cells at practical emitter temperatures.

The dependence of efficiency upon cell thickness and blackbody temperature is a result of four competing factors. Firstly, increasing cell thickness and blackbody temperature increases J_{sc} due to greater absorption and a better optical match to the bandgap of silicon. Counteracting this effect is increased carrier transport losses to the rear surface for greater cell thicknesses, and larger losses resulting from the thermalisation of carrier energy following absorption of high-energy photons for higher blackbody temperatures. For greater cell thicknesses and lower blackbody temperatures there is a proportionally higher loss of sub-bandgap photons due to parasitic free carrier absorption. There is a small decrease in efficiency for low cell thicknesses due to thermalisation loss associated with the relatively larger number of high-energy photons absorbed compared with thicker cells. This is a result of the absorption profile of silicon—high absorption for short photon wavelengths, decreasing exponentially for longer wavelengths. Thin cells absorb proportionally more high-energy photons than thicker cells, resulting in proportionally higher thermalisation losses. This effect was observed with the additional study of different antireflectance schemes, whereby poorly utilised high-energy photons can be preferentially returned to the emitter.

Alongside TPV efficiency, it is also important to consider TPV system output power density, since low output power density implies a larger and more costly cell array.

From Fig. 6 we observe that resistive losses are the primary limiting factors for cell performance in TPV systems. The vertical

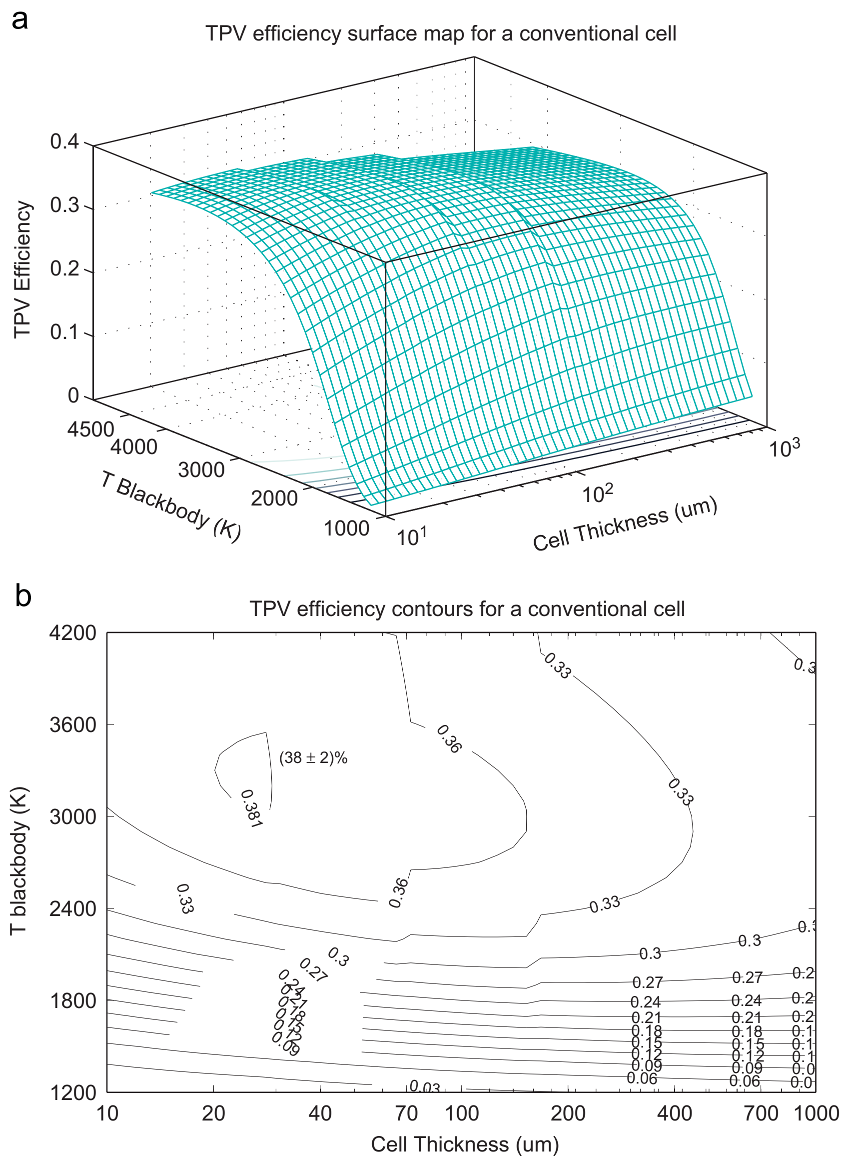

Fig. 5. (a) Conventional cell TPV efficiency surface. (b) Conventional cell TPV efficiency contour map. A broad maximum for low cell thicknesses and relatively high blackbody temperatures is observed. The small discontinuities are an artifact resulting from progressively changing the material resistivity to ensure high IQE.

contours indicate that optimal J_{sc} is dependent on cell thickness, that is, the distance between the blackbody and cells is adjusted for each cell thickness to ensure J_{sc} is at its optimal value, balancing volume recombination and transport resistive losses. It is from this analysis that we find that the primary advantage for thin conventional cells is due to decreased resistance, and not lower levels of free-carrier absorption. This was contrary to initial expectation.

3.2. *Sliver cells*

A similar analysis to the above was performed for sliver cells. Sliver cells were modelled with a 1% wavelength-independent optical loss to account for the small metal contact surface area at the edges of each cell. Sliver cell widths were limited to a minimum of 300 μm. The same mirror reflectances and antireflection coatings as for the conventional cells were applied, and sliver cell temperature was likewise modelled at 318 K (Fig. 7).

Similar to conventional cells, a broad efficiency maximum for high blackbody temperatures is observed. In contrast to conventional cells, the maximum occurs for *large* cell thicknesses, although the dependence upon thickness is quite weak. This is due to the transport resistance of holes in sliver cells being inversely proportional to cell thickness. The main limiting factor for sliver cell performance was identified to be lateral resistance loss of electrons within the cell's emitter, which is not dependent upon cell thickness. The minimum resistance was set to 40 Ω/sq. Emitter sheet resistance could be further reduced to reduce resistive losses, at the cost of reduced blue response (which is of lesser importance for lower thermal emitter temperatures) and increased recombination.

Sliver cell relative maximum efficiencies were found to be ~85% of those achieved by conventional cells. This difference is larger than the uncertainty range of the model. However, at a practical emitter temperature of 2000 K, sliver cell efficiencies are approximately equivalent to conventional cell efficiencies at 2000 K, at ~27%.

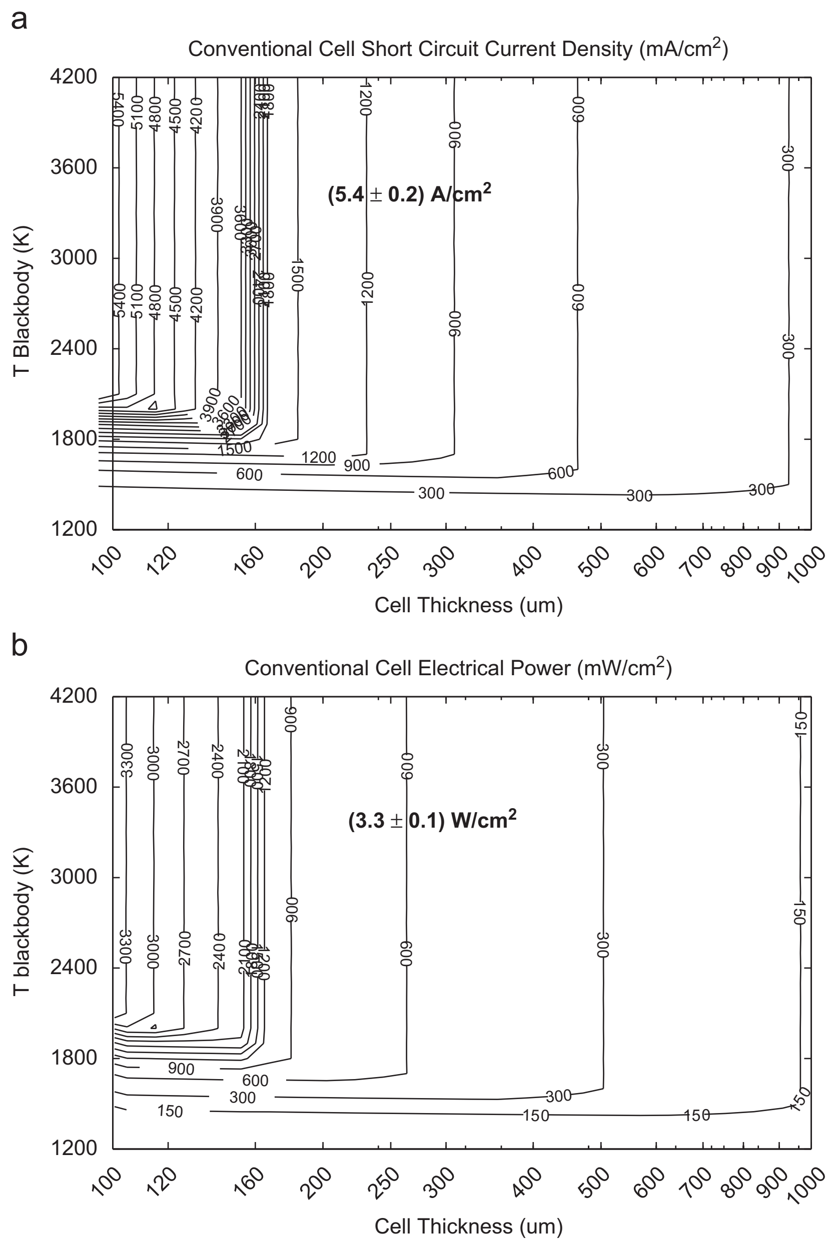

Fig. 6. (a) Short-circuit current density and (b) electrical power output densities for a conventional cell in a TPV system. High output power densities are observed for thin cells.

Again it is instructive to examine the output power density contours. In Fig. 8 it is observed that electrical output densities for the optimum cell design are a factor of 5 times *lower* than that for conventional cells due to lateral resistive losses. The importance of this potential disadvantage for sliver cells in TPV systems depends on the cost of silicon cells relative to that of the whole TPV system. To overcome this limitation, sliver cell widths could be reduced. Due to emitter resistances depending on the square of sliver cell *width*, halving sliver width would result in a fourfold reduction in lateral resistive losses. Halving sliver width would present additional challenges of increased metal contact area, reduced packing density and a doubling of the number of wafers and slivers that need to be handled per TPV system. On the other hand, it would allow for a doubling of the rate at which voltage builds across the sliver module and the current halves, reducing resistive losses. The feasibility of this approach is a subject of current research.

3.3. Extra TPV considerations

Alongside cell efficiency and electrical power output considerations for TPV systems are the practical design issues of heat-sinking, non-uniform irradiation by the thermal emitter, and cell interconnection.

Cell temperature is an important consideration for TPV systems [3]. Additional modelling indicated that temperature is of equal importance as spectral filtering, confirming earlier studies. That sliver cells have their contacts on the sides of the cell is an advantage for heat sinking; thermally conducting material with an integrated mirror can be bonded directly to the back surface of the cell without allowance for electrical isolation of electrical contacts. This allows for excellent low-cost heat sinking. For back-contact cells, heat sinking is more difficult. The back surface must accommodate the mirror, the electrical contacts and the electrical conductors while maintaining a low

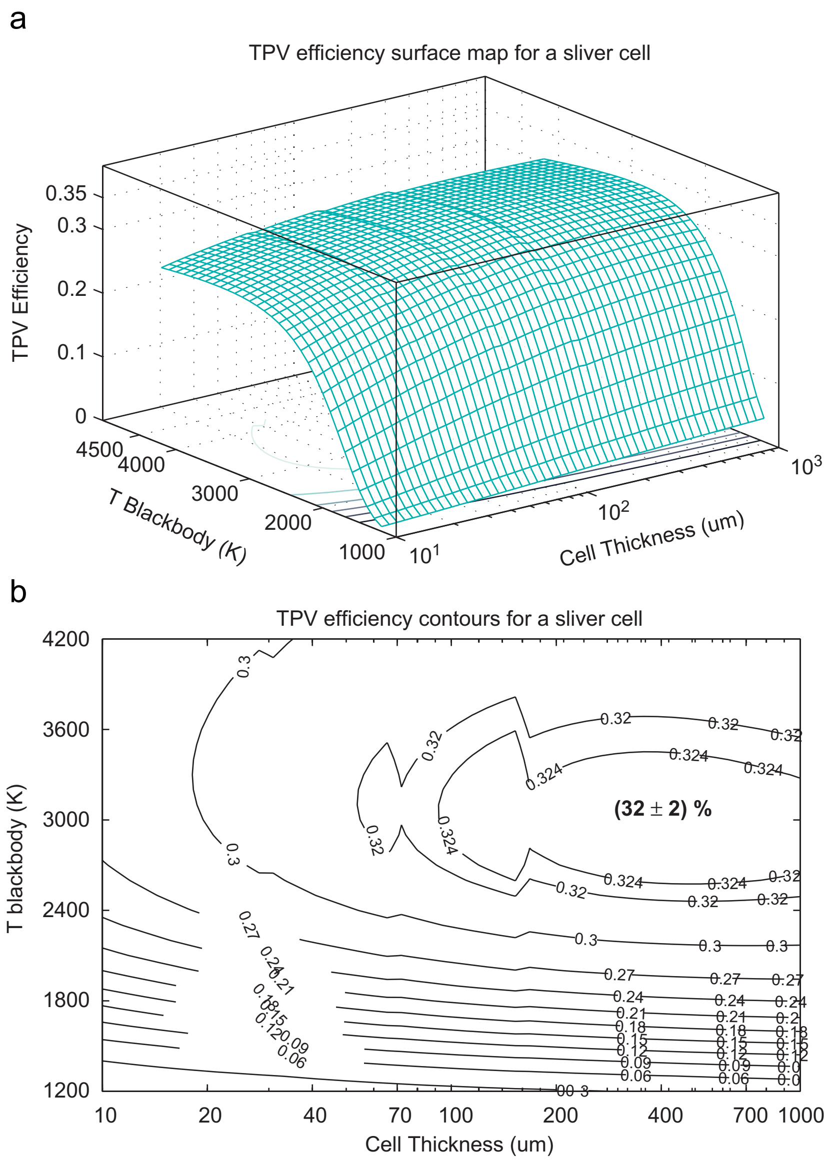

Fig. 7. (a) Sliver cell efficiency surface and (b) sliver cell efficiency contour map. A broad efficiency maximum for *large* cell thickness is observed. The small discontinuities are an artifact resulting from progressively changing the material resistivity to ensure high IQE.

risk of shorting between n and p contacts. The electrical contacts and conductors must also be designed to achieve low obscuration of sub-bandgap photons.

Another significant issue for TPV systems is non-uniform radiation by the thermal emitter. This poses problems for the circuit design of cells in a TPV system. The narrow width of sliver cells allows for cells to be easily series connected to form small high-voltage submodules, which are then connected in parallel. In addition, sliver cells can be readily designed to have a very low reverse breakdown voltage by careful control of the doping profile of adjacent diffused regions, which obviates the need for bypass diodes. External circuit resistances will be significantly lower for sliver modules than conventional modules due to the high voltage and low current of each submodule.

The above considerations of heat-sinking, non-uniform irradiation and cell interconnection favour sliver cell geometries for practical TPV systems, and will offset the higher resistive losses of sliver cells. However, real TPV systems have many losses not considered in this paper [14]. Complete manufactured TPV systems utilising silicon solar cells and fossil fuel heating of the emitter have reported net system electrical efficiencies of 4.5–7.5% [15]. Careful and innovative engineering will be required to produce TPV systems with attractive efficiencies compared with alternative methods of electricity generation.

4. Conclusions

Within the range of parameters examined, it was found that sliver cells do not offer an efficiency advantage over well-designed conventional cells in TPV systems. The model indicated that high illumination intensities are desirable in order to take advantage of higher open-circuit voltages, to be achieved by placing cells close to the emitter. Sliver cell output power densities at these illumination intensities were observed to be strongly limited by lateral transport resistance. This is due to sliver contacts being at the edges of the cell, resulting in resistive power losses that vary as the square of cell width. Minimum sliver cell widths in this study were limited to 300 μm. As a result, series resistance losses

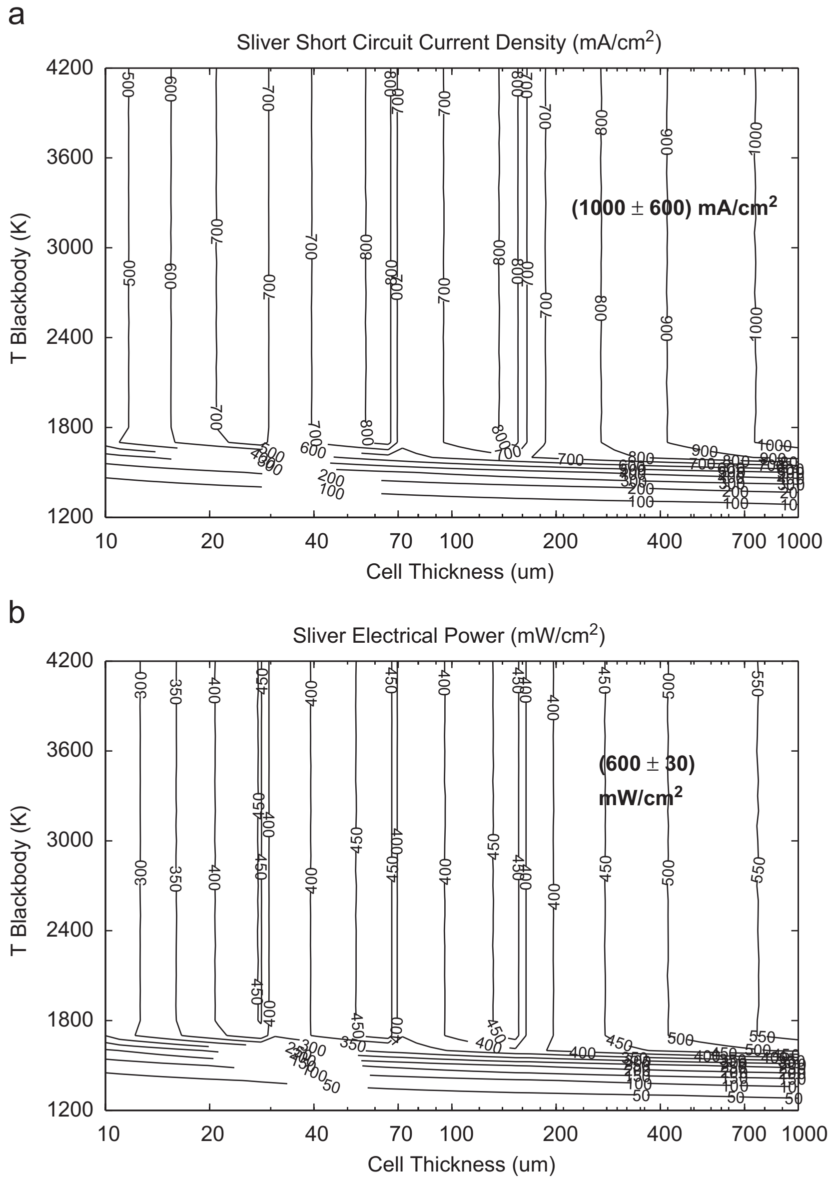

Fig. 8. (a) Sliver cell TPV short-circuit current density and (b) electrical power output density. The relatively broad maximum is due to sliver cell performance being limited by cell width, which were held constant at 300 μm for all cell thicknesses. The maximum for *large* cell thicknesses is due to resistive losses being inversely proportional to cell thickness.

for sliver cells were found to be significantly higher than for thin conventional cells with vertical carrier transport.

Within the assumptions of the model, sliver cell maximum efficiencies (32 ± 2)% were found to be ~85% of the maximum efficiency achieved by conventional cells (38 ± 2)%. At practical TPV temperatures of ~2000 K, the modelled efficiencies of sliver and conventional cells were quite similar at 27%. Sliver cell maximum output power densities (~600 mW/cm^2) were substantially lower than those for conventional cells (~3300 mW/cm^2). Current research is examining the feasibility of narrow sliver cells with lower lateral resistive losses.

Practical considerations of heat sinking, submodule resistances and metal contact area at high incident power densities are likely to favour sliver cell geometries.

Neglecting the practical considerations mentioned above, optimal cells for TPV systems were found to be thin back-contact cells with spectral filtering that reflected high-energy photons back to the emitter. The primary advantage for thin cells in TPV systems was observed to be a result of decreased transport losses rather than spectral considerations. This was contrary to initial expectation.

Modelled cells were composed of silicon. Silicon cells were found to perform best at emitter temperatures that are well above the current range of feasibility for TPV systems. The cost advantages of silicon over other semiconductor materials may be offset by increased costs due to high emitter operating temperatures and the resulting need for very good emitter materials and cooling systems.

Acknowledgments

Niraj Lal would like to thank the community at the ANU Centre for Sustainable Energy Systems, and in particular Dr. Evan Franklin who provided valuable assistance with programming. Niraj Lal also acknowledges the support of the ANU Angus Nicholson Scholarship.

References

[1] A. DeVos, Endoreversible Thermodynamics of Solar Energy Conversion, Oxford University Press, Oxford, 1992.
[2] N. Harder, P. Wurfel, Theoretical limits of thermophotovoltaic solar energy conversion, Semicond. Sci. Technol. 18 (5) (2003) S151–S157.
[3] T. Coutts, An overview of thermophotovoltaic generation of electricity, Sol. Energy Mater. Sol. Cells 66 (2001) 443–452.
[4] D. Martin, C. Algora, Key issues for an accurate modelling of GaSb TPV converters, in: Fifth Conference on TPV Generation of Electricity, 2002, pp. 442–451.
[5] R.M. Swanson, Silicon photovoltaic cells in thermophotovoltaic energy conversion, International Electron Devices Meeting, vol. 18, no. 5, 1978, pp. 70–73.
[6] A. Blakers, K. Weber, et al., Sliver cells – a complete photovoltaic solution, in: IEEE fourth World PV Energy Conference Proceedings, 2006.
[7] E. Franklin, V. Everett, A. Blakers, K. Weber, "Sliver Solar Cells: High-Efficiency, Low-Cost PV Technology" Adv. OptoElectron. 2007 (2007) (Article ID 35383).
[8] J. Aschaber, et al., Realistic modelling of TPV systems, Semicond. Sci. Technol. 18 (5) (2003) S156–S164.
[9] National Astronomical Observatory of Japan Website, accessed August 2008, 〈http://www.naoj.org/Observing/Telescope/Parameters/Reflectivity〉.
[10] D. Boufhas, et al., Design and simulation of antireflection coating systems for optoelectronic devices: application to silicon solar cells, Sol. Energy Mater. Sol. Cells 52 (1998) 79–93.
[11] L. Fraas, et al., Thermophotovoltaic system configurations and spectral control, Semicond. Sci. Technol. 18 (5) (2003) S165–S173.
[12] M. Green, Solar Cells, Prentice-Hall, New Jersey, 1986.
[13] D. Clugston, P. Basore, PC1D version 5: 32-bit solar modelling on personal computers, in: 26th IEEE PV Specialists Conference, 1997, pp. 207–210.
[14] R. Mahorter, et al., Thermophotovoltaic system testing, Semicond. Sci. Technol. 18 (5) (2003) S232–S238.
[15] F.E. Becker, et al., Development of a portable thermophotovoltaic power generator, in: Proceedings of the Third NREL Conference on Thermophotovoltaic Generation of Electricity, March 1997, vol. 401, AIP Conf. Proc. (1997), pp. 329–339.